Available online at www.sciencedirect.com
SCIENCE DIRECT®
Journal of Catalysis 225 (2004) 37–44
JOURNAL OF CATALYSIS
www.elsevier.com/locate/jcat

Mechanistic and kinetic insights into N_2O decomposition over Pt gauze

V.A. Kondratenko * and M. Baerns *

Institute for Applied Chemistry Berlin–Adlershof, Richard-Willstätter-Str.12, D-12489 Berlin, Germany

Received 9 December 2003; revised 26 March 2004; accepted 29 March 2004

Available online 30 April 2004

Abstract

Mechanistic and kinetic aspects of the catalytic decomposition of N_2O over knitted Pt gauze were studied by transient experiments in vacuum using the temporal analysis of products (TAP-2) reactor in the temperature range from 573 to 1073 K. At temperatures above 773 K N_2O decomposes resulting in the formation of gas-phase oxygen and nitrogen. Gas-phase oxygen was shown to inhibit N_2O decomposition over the gauze for all temperatures studied. The transient responses of N_2O as well as products of its decomposition (N_2 and O_2) were simultaneously fitted to different kinetic models. Through model discrimination it was shown that molecular oxygen is formed only via interaction of N_2O with adsorbed oxygen atoms, originating from the interaction of N_2O with metallic Pt sites, as it was speculatively proposed earlier by Riekert and co-workers [Z. Electrochem. 66 (1962) 735; Ben. Bunsen-Ges. Phys. Chem. 67 (1963) 976; Proc. 3rd Intl. Congr. Catal. 1 (1965) 387]. The formation of molecular oxygen via recombination of two surface oxygen atoms was assumed to be slow under transient vacuum conditions as compared to ambient pressure steady-state conditions, due to a lower coverage by these oxygen species. The reaction scheme was supported by results of oxygen-isotopes experiments.

Keywords: TAP reactor; Decomposition of N_2O; N_2O; Kinetics; Pt catalyst; Pt gauze

1. Introduction

Recently the environmental impact of N_2O has attracted strong public attention because of its assumed contribution to global warming and ozone depletion in the upper atmosphere. The annual emission of N_2O was estimated to be 4.7 to 7×10^6 tons [1]. The increase of the atmospheric N_2O content in the last century has been attributed to various anthropogenic sources [2]. The main sources identified include adipic acid production, the combustion of fossil fuels, and biomass, land cultivation, and nitric acid production [3]. In the latter process N_2O is formed as by-product of high-temperature oxidation of ammonia to nitric oxide with air over Pt–Rh alloys, used in the form of gauze packs. Although the ammonia oxidation reaction is a highly optimized industrial process, the mechanism of formation and decomposition of N_2O has to be better understood, in order to possibly suppress N_2O formation and hence, to reduce environmental pollution by N_2O.

According to previous studies on N_2O decomposition over differently structured Pt catalysts (wires [4–10], foils [5,6], and sponges [11]), Pt is active for N_2O decomposition. Two different mechanisms of N_2O decomposition have been suggested. Hinshelwood et al. [4] proposed that N_2O adsorbs reversibly on the catalyst surface [Eq. (1)] followed by irreversible decomposition of adsorbed N_2O [Eq. (2)] with the formation of gas-phase molecular nitrogen and an adsorbed atomic oxygen species. Gas-phase oxygen is then formed via reversible recombination of the adsorbed oxygen species [Eq. (3)].

$$N_2O + s \rightleftarrows N_2O\text{–}s, \tag{1}$$

$$N_2O\text{–}s \rightarrow N_2 + O\text{–}s, \tag{2}$$

$$2O\text{–}s \rightleftarrows O_2 + 2s. \tag{3}$$

Later, Schmidt's group [9,10] used this mechanistic scheme for fitting experimental data obtained in a wide range of pressures and temperatures under steady-state conditions. It was shown that the rate of N_2O decomposition could be

* Corresponding authors. Fax: +49 30 63924454 (V.A. Kondratenko), +49 30 63924454 (M. Baerns).
E-mail addresses: viko@aca-berlin.de (V.A. Kondratenko), baerns@aca-berlin.de (M. Baerns).

0021-9517/$ – see front matter
doi:10.1016/j.jcat.2004.03.038

fitted with an accuracy of ±15% under the experimental conditions.

An alternative mechanism for N_2O decomposition over Pt wire [Eqs. (4)–(7)] has been proposed by Riekert and co-workers [6]. This mechanism assumes N_2O decomposition over Pt atoms forming molecular nitrogen and adsorbed oxygen species [Eq. (4)]. The reaction of N_2O with these adsorbed oxygen species leads to the formation of molecular oxygen and nitrogen [Eq. (5)].

$$N_2O + s \rightarrow N_2 + O\text{–}s, \quad (4)$$

$$N_2O + O\text{–}s \rightarrow N_2 + O_2 + s, \quad (5)$$

$$O_2 + s \rightleftarrows O_2\text{–}s, \quad (6)$$

$$O_2\text{–}s + s \rightarrow 2O\text{–}s. \quad (7)$$

The two above reaction mechanisms differ in the reaction pathways for oxygen formation. According to the first mechanism [Eqs. (1)–(3)], gas-phase oxygen is formed via reversible recombination of adsorbed oxygen atoms [Eq. (3)], while for the second model [Eqs. (4)–(7)] the interaction of gas-phase N_2O with adsorbed oxygen atoms [Eq. (5)] is the only source of O_2 formation. However, the latter mechanism is based on studies, which have been done in static reactors using either Pt wires or foils. These results might be complicated by separation between intrinsic chemical kinetics and transport phenomena. Therefore, in order to derive more detailed mechanistic insights into N_2O decomposition, a transient technique (TAP reactor) was applied in combination with an isotopic technique for studying the decomposition of N_2O over an industrially relevant knitted Pt gauze catalyst.

2. Experimental

2.1. Catalytic material

Knitted gauze made of polycrystalline Pt (Multinit type 4) wire was supplied by Degussa. Its BET surface area amounted to 0.002 $m^2\,g^{-1}$; for these measurements Kr was used as adsorbent because of the low surface area.

XPS measurements have shown that the catalyst contained some traces of Zn and Pb, which were segregated on its surface with surface concentration of 1 and 0.3%, respectively. Carbon was, however, the main impurity. It could be almost completely removed after pretreatment in oxygen flow.

2.2. Transient experiments

Transient experiments were carried out in the TAP-2 reactor system, which has been described elsewhere [12,13]. The Pt gauze (0.119 g) was packed (packing density 4.2×10^3 $kg\,m^{-3}$) between two layers of quartz particles (d_p = 250–355 μm) in the isothermal zone of the quartz-made microreactor (d = 6 mm, L = 40 mm).

Before the transient experiments the Pt gauze was pretreated at ambient pressure in a flow of oxygen (30 $ml\,min^{-1}$) at 1073 K for 60 min to remove carbon deposits. After this pretreatment the Pt gauze was exposed to vacuum conditions (10^{-8} mbar). For pulse experiments the temperature of the catalyst was set to a desired value from 1073 to 573 K stepwise by 100 K, starting from the pretreatment temperature. For isotopic transient experiments the Pt gauze was pretreated by pulsing $^{18}O_2$ at the desired reaction temperature followed by pulsing of nonlabeled oxygen or N_2O. The total pulse size was kept below 10^{15} molecules in order to stay in the Knudsen-diffusion regime and suppress any gas-phase reactions. Under such conditions, only interactions between gas-phase molecules and Pt gauze took place. Transient responses were recorded by pulsing $N_2O/Xe/Ne = 1/1/1$, $N_2O/O_2/Ne = 1/1/1$, $N_2O/Ne = 1/1$, and $O_2/Ne = 1/1$ mixtures at atomic mass units (AMUs) related to N_2O (44.0, 30.0, 28.0), reaction products, that is, $^{18}O_2$ (36.0), $^{18}O^{16}O$ (34.0) (for isotopic experiments), $^{16}O_2$ (32.0), N_2 (28.0), inert gas Ne (20.0), and Xe (132.0) at the reactor outlet. For each AMU, pulses were repeated 10 times and averaged to improve the signal-to-noise ratio.

2.3. Treatment of TAP data

For the evaluation of mechanistic and kinetic data on N_2O decomposition, the transient responses of N_2O, O_2, and N_2 were fitted to different kinetic models. The fitting procedure was based on a numerical solution of partial differential equations describing the processes of diffusional transport, adsorption, as well as desorption of reactants and the catalytic reaction on the catalyst within the reactor. The software code used allows a simple implementation of different models without any restriction on the number of reaction steps [14,15].

The diffusional transport through the reactor, which is quantitatively described in a partial differential equation for each gas-phase molecule [14], was characterized through the quality of fitting of the transient response of Ne to the model, assuming Knudsen diffusion only (Fig. 1). The effective diffusion coefficient of Ne as estimated from this fitting was used as a fixed parameter for further calculations of the effective diffusion coefficients of other gas-phase species according to $D_A^{eff} = D_{Ne}^{eff}\sqrt{M_{Ne}/M_A}$ in the further fitting applying different kinetic models. As a criterion for the quality of fitting the residual was calculated according to $\text{residual} = \sqrt{\frac{1}{N}\sum_{i=1}^{N} r_i^2}$, where r_i is the shortest deviation between the representative points of experimental and simulated responses and N is the number of these points. The residual of fit assuming Knudsen diffusion only (Fig. 1) was 1.62×10^{-3}, i.e. considerably lower than that for the more complex kinetic models (Table 1).

In our modeling procedure, the units of the rate of reaction with gas-phase molecules are $mol\,m_{cat}^{-3}\,s^{-1}$, while those

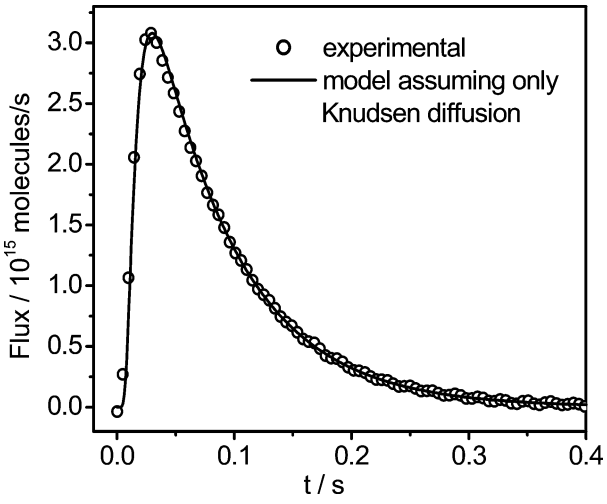

Fig. 1. Comparison between experimental (o) and simulated (—) responses of Ne at 973 K assuming Knudsen diffusion only ($D_{Ne}^{eff} = 1.08 \times 10^{-2}$ m^2 s^{-1}).

of surface species only are mol m_{cat}^{-2} s^{-1}. The concentration of gas phase and surface species are expressed in mol m_{cat}^{-3} and mol m_{cat}^{-2}, respectively.

3. Results

3.1. N_2O decomposition and the role of oxygen

Transient experiments have shown that N_2O decomposition starts above 673 K. N_2 and O_2 were the only observed gas-phase products detected at the reactor outlet. The temperature dependences of the molar fractions of N_2O, N_2, and O_2 are shown in Fig. 2 (solid symbols). Thermal decomposition of nitrous oxide did not exceed 5% at 1073 K in the reactor filled with quartz only as compared to 77% in the presence of catalyst.

In order to check if gas-phase oxygen influences N_2O decomposition under vacuum conditions, transient experiments were performed at different temperatures using a $N_2O/O_2 = 1/1$ mixture diluted by neon. The N_2O concentration was ca. 30 vol% in the feed mixture without and with added oxygen. The experimental data are presented in Fig. 2 (open symbols). The degree of N_2O decomposition and the amount of N_2 formed decrease slightly when oxygen is added to the nitrous oxide. This indicates that oxygen and N_2O compete for the same active sites, hereby oxygen inhibits partly the decomposition of N_2O over Pt gauze.

3.2. Kinetic and mechanistic evaluation of N_2O decomposition

In order to derive probable mechanistic insights from kinetics into the decomposition of N_2O particularly with respect to oxygen formation at high temperatures (873–1073 K), transient responses of both N_2O and reaction products (O_2 and N_2) were simultaneously fitted to 7 different kinetic models (see Table 1). These kinetic models were chosen taking into account literature data on N_2O decomposition over polycrystalline platinum Pt [6,7,10,16], Rh black [17], and Pd (110) single crystal [18]. The choice was not restricted to the two models, as described in the introduction in order to provide an unprejudiced data examination. The models were applied in the order of increasing their complexity.

The elementary reaction steps implicated in these models were chosen according to the results of our own and previously reported experiments. Thus, decomposition of N_2O via an adsorbed molecular intermediate N_2O–s [Eq. (2)] was not taken into consideration since according to Avery [19] N_2O desorbs completely from a Pt (111) surface at temper-

Table 1
Kinetic models used for fitting of experimental data on N_2O decomposition over Pt at 973 K

Reaction steps	Model number	Best residual
$N_2O + s \xrightarrow{k_1} N_2 + O\text{–}s$ $N_2O + O\text{–}s \xrightarrow{k_2} N_2 + O_2 + s$	1	1.05×10^{-1}
$N_2O + s \xrightarrow{k_1} N_2 + O\text{–}s$ $2O\text{–}s \xrightarrow{k_2} O_2 + 2s$	2	5.00×10^{-2}
$N_2O + s \xrightarrow{k_1} N_2 + O\text{–}s$ $2O\text{–}s \underset{k_3}{\overset{k_2}{\rightleftarrows}} O_2 + 2s$	3	4.09×10^{-2}
$N_2O + s \xrightarrow{k_1} N_2 + O\text{–}s$ $N_2O + O\text{–}s \xrightarrow{k_2} N_2 + O_2 + s$ $2O\text{–}s \xrightarrow{k_3} O_2 + 2s$	4	2.97×10^{-2}
$N_2O + s \xrightarrow{k_1} N_2 + O\text{–}s$ $N_2O + O\text{–}s \xrightarrow{k_2} N_2 + O_2 + s$ $2O\text{–}s \underset{k_4}{\overset{k_3}{\rightleftarrows}} O_2 + 2s$	5	3.19×10^{-2}
$N_2O + s \xrightarrow{k_1} N_2 + O\text{–}s$ $N_2O + O\text{–}s \xrightarrow{k_2} N_2 + O_2 + s$ $2O\text{–}s \underset{k_4}{\overset{k_3}{\rightleftarrows}} O_2\text{–}s + s$ $O_2\text{–}s \underset{k_6}{\overset{k_5}{\rightleftarrows}} O_2 + s$	6	2.29×10^{-2} insensitive to k_3
$N_2O + s \xrightarrow{k_1} N_2 + O\text{–}s$ $N_2O + O\text{–}s \xrightarrow{k_2} N_2 + O_2 + s$ $O_2 + s \underset{k_4}{\overset{k_3}{\rightleftarrows}} O_2\text{–}s$ $O_2\text{–}s + s \xrightarrow{k_5} 2O\text{–}s$	7	1.14×10^{-2}
$N_2O + s \xrightarrow{k_1} N_2 + O\text{–}s$ $N_2O + O\text{–}s \xrightarrow{k_2} N_2 + O_2\text{–}s$ $O_2\text{–}s \underset{k_4}{\overset{k_3}{\rightleftarrows}} O_2 + s$ $O_2\text{–}s + s \xrightarrow{k_5} 2O\text{–}s$	8	1.50×10^{-2}

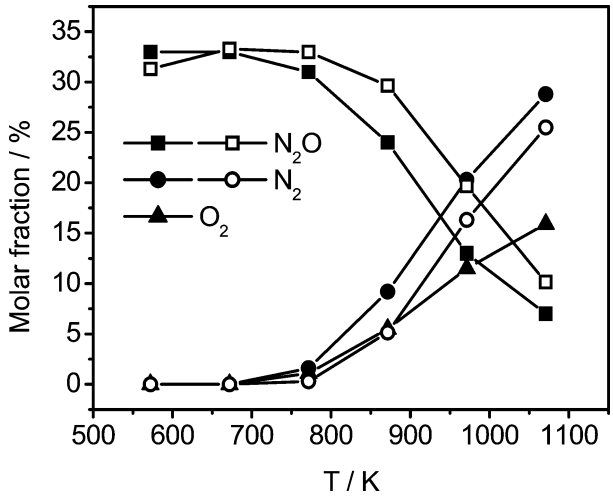

Fig. 2. Molar fractions of N_2O, O_2, and N_2 on pulsing N_2O/Xe/Ne = 1/1/1 (solid symbols) and N_2O/O_2/Ne = 1/1/1 (open symbols) mixtures at different temperatures over Pt gauze.

atures of 90–105 K. No adsorption of nitrous oxide was also observed over Pt sponge at 523 K [20]. Moreover, our results on N_2O pulsing at lower temperatures provide no evidence for measurable adsorption of N_2O on Pt gauze. Based on the above observations no adsorbed N_2O species were included in all the models. A direct reactive interaction of gas-phase N_2O with metallic surface sites [Eq. (4)] was assumed as the first reaction step for each model.

The experimental and simulated transient responses of N_2O, O_2, and N_2 assuming models 1 to 3 are shown in Fig. 3. The models differ in the reaction pathways of oxygen formation. Although they describe the experimental data for N_2O and N_2 well (Fig. 3), no fully satisfactory description for the transient response of oxygen was achieved. Models 2 and 3, which assume formation of gas-phase oxygen via recombination of adsorbed oxygen atoms, describe the experimentally observed O_2 tailing better than model 1. However, maxima of the simulated oxygen transient responses are shifted to extended times in comparison to the maximum of the experimental curve. In contrast to models 2 and 3, model 1 describes the maximum of the experimental transient response of oxygen perfectly. Thus, it is suggested that formation of molecular oxygen could take place by interaction of adsorbed oxygen atoms with N_2O as well as their recombination. At low surface coverage by atomic oxygen, formation of molecular oxygen occurs via interaction of nitrous oxide with adsorbed oxygen atoms. With an increase in coverage, recombination of two atomic oxygen species begins to play an important role in oxygen formation, since this reaction step is of second order with respect to adsorbed atomic oxygen.

Models 4 and 5 take the above assumption into account; Fig. 4 gives a comparison of the experimental and simulated transient responses of N_2O and products of its decomposition. Both models describe the experimental data better than models 1–3, but the description of the oxygen transient response was still not satisfactory. This is especially valid for its maximum and tailing. The regularity of the observed deviation between the experimental and simulated data indicates the inadequacy of these models. Besides, these models do not describe the transient responses of N_2O, O_2, and N_2 over the whole temperature range (873–1073 K), when the data were fitted simultaneously. Therefore, a new extended model was taken into consideration. This model (No. 6) considers participation of adsorbed molecular oxygen species, as previously suggested by Riekert et al. [6] as an intermediate in oxygen dissociation. Actually, model 6 gives a better fit of the transient responses of N_2O, N_2, and O_2 than the above models. The recombination of two adsorbed atomic oxygen species, however, had to be rejected, since the objective function was insensitive to this parameter. This can be ascribed to the experimental vacuum transient conditions, at which coverage by adsorbed atomic oxygen species, formed from N_2O, is low due to the small amounts of N_2O pulsed. Therefore, recombination of adsorbed oxygen species, which is a reaction of second order, is slow and its influence on the shape of the oxygen transient response is negligible. Thus, model 6 was modified by excluding the reaction step, which describes the recombination of adsorbed oxygen atoms. The respective model 7 (Fig. 5) assumes de-

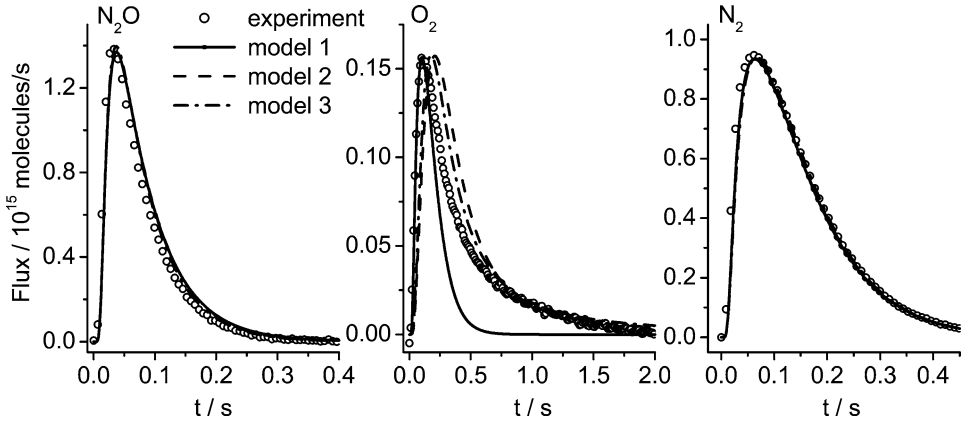

Fig. 3. Comparison between experimental (o) and simulated (—) responses of N_2O, O_2, and N_2 during N_2O decomposition at 973 K. (Fitting based on kinetic models 1–3.)

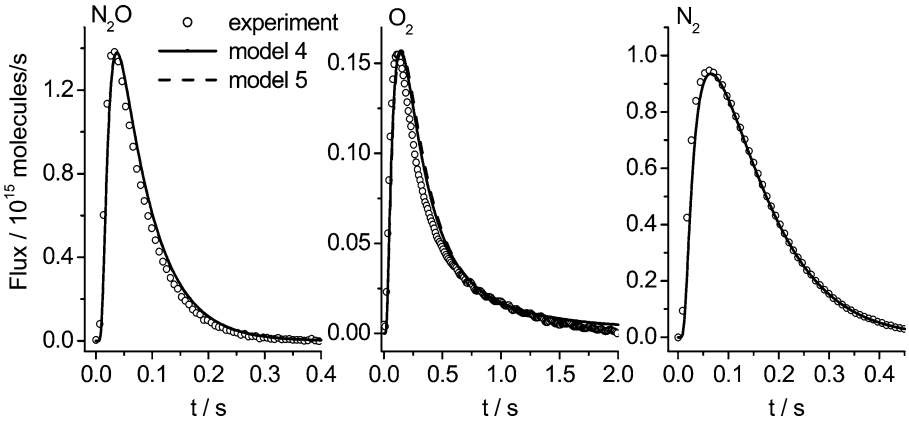

Fig. 4. Comparison between experimental (o) and simulated (—) responses of N_2O, O_2, and N_2 during N_2O decomposition at 973 K. (Fitting based on kinetic models 4 and 5.)

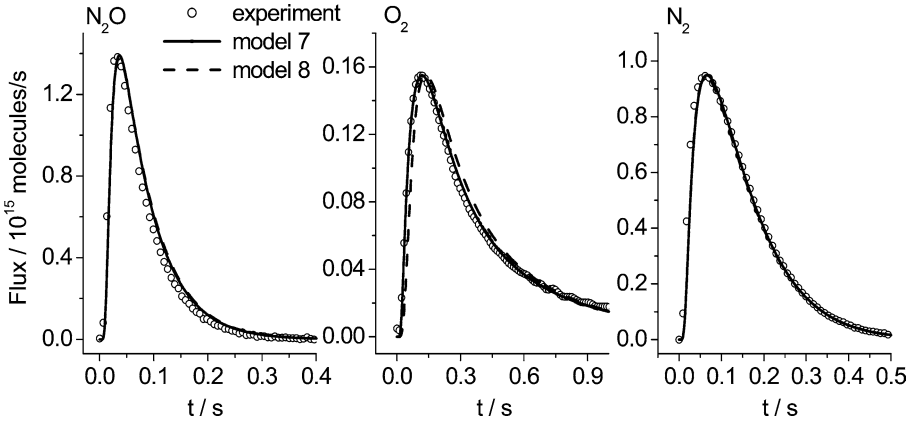

Fig. 5. Comparison between experimental (o) and simulated (—) responses of N_2O, O_2, and N_2 during N_2O decomposition at 973 K. (Fitting based on kinetic models 7 and 8.)

composition of N_2O on reduced metallic sites to molecular nitrogen and adsorbed oxygen atoms, which can also interact with N_2O, yielding gas-phase molecular oxygen and nitrogen. Gas-phase molecular oxygen, in turn, can be reversibly adsorbed and dissociate to O–s. Thus, this model assumes two elementary steps, which lead to gas-phase oxygen: O_2–s $\rightarrow$ $O_2 + s$ and $N_2O + O\text{–}s \rightarrow N_2 + O_2 + s$. Based on kinetic parameters derived from the fitting, the fractional coverage by atomic oxygen species is estimated to be 0.6% of the total number of surface Pt atoms. In order to elucidate the way of gas-phase oxygen formation, it was assumed in model 8, that interaction of N_2O with O–s leads to the formation of adsorbed molecular oxygen species. The formation of gas-phase oxygen occurs then only via desorption. The results of fitting the experimental data to the latter model are shown in Fig. 5. It can be seen, that excluding of the step, which describes direct formation of gas-phase oxygen via $N_2O + O\text{–}s \rightarrow N_2 + O_2 + s$, leads to a shift of the simulated curve to the extended times and to worsening of the description of the oxygen transient response.

Based on the results of model discrimination at the reference temperature of 973 K, model 7 (see Table 1), which provides the best description of experimental data, was selected for simultaneous fitting the transient responses of N_2O and products of its decomposition (N_2 and O_2) at all temperatures (873–1073 K). Activation energies could be derived for all the reaction steps according to

$$k_i = k_{T_{\text{ref}}} \exp\left(-\frac{E_a}{R}\left(\frac{1}{T_i} - \frac{1}{T_{\text{ref}}}\right)\right), \tag{8}$$

where T_{ref} is a reference temperature at which $k_{T_{\text{ref}}}$ were initially obtained from fitting.

A good description of the transient data was obtained for each temperature. The activation energies and reaction-rate constants at the reference temperature are presented in Table 2.

For further confirmation or rejection of the evaluated reaction mechanism of oxygen formation in N_2O decomposition over Pt gauze, an isotopic exchange technique was applied. The results are presented and discussed below.

3.3. Transient isotopic experiments

On pulsing $N_2{}^{16}O$ over Pt gauze precovered by ^{18}O species during the pretreatment in $^{18}O_2$, the oxygen isotopes

Table 2
Kinetic parameters of model 7 for N_2O decomposition over oxygen-pretreated Pt gauze at 873–1073 K

Reaction step	k_i ($T = 973$ K)	E_a (k_i) kJ mol^{-1}
$N_2O + s \xrightarrow{k_1} N_2 + O\text{–}s$	2.0×10^8 m^2_{cat} mol^{-1} s^{-1}	81
$N_2O + O\text{–}s \xrightarrow{k_2} N_2 + O_2 + s$	9.5×10^9 m^2_{cat} mol^{-1} s^{-1}	173
$O_2 + s \xrightarrow{k_3} O_2\text{–}s$	1.9×10^9 m^2_{cat} mol^{-1} s^{-1}	21
$O_2\text{–}s \xrightarrow{k_4} O_2 + s$	1.2×10^1 s^{-1}	10
$O_2\text{–}s + s \xrightarrow{k_5} 2O\text{–}s$	4.3×10^5 m^2_{cat} mol^{-1} s^{-1}	31

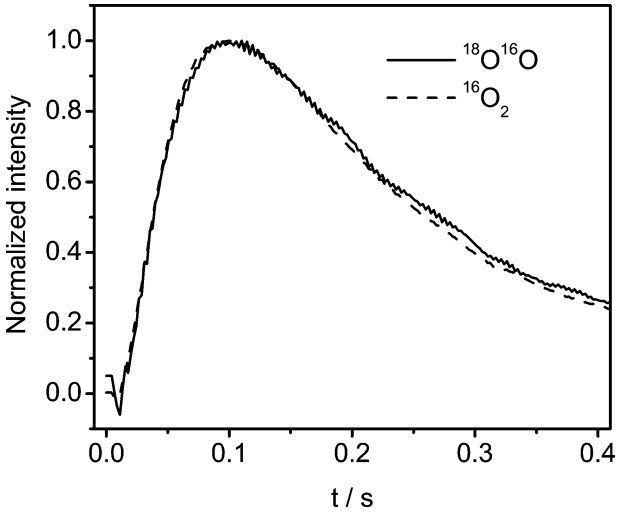

Fig. 6. Normalized transient responses of $^{18}O^{16}O$ and $^{16}O_2$, formed in $N_2{}^{16}O$ decomposition at 973 K over Pt gauze pretreated by $^{18}O_2$.

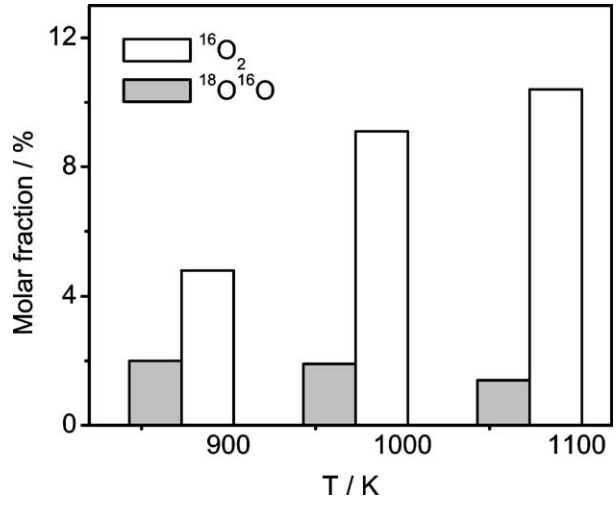

Fig. 7. Molar fractions of $^{16}O_2$ and $^{18}O^{16}O$ isotopes, formed in $N_2{}^{16}O$ decomposition at different temperatures over Pt gauze pretreated by $^{18}O_2$.

observed were $^{16}O_2$ and $^{16}O^{18}O$, the former being the main reaction product. The shapes of the normalized transient responses of $^{16}O_2$ and $^{16}O^{18}O$ are nearly the same as shown on Fig. 6. This indicates that both isotopes are formed via the same reaction pathway. The distribution of oxygen isotopes as a function of temperature is shown in Fig. 7. It can be seen that an increase in the molar fraction of $^{16}O_2$ formed from N_2O is accompanied by a slight decrease in the molar fraction of labeled oxygen ($^{16}O^{18}O$).

For examining the influence of a secondary isotopic exchange of oxygen on the interpretation of the interaction of N_2O with ^{18}O pretreated Pt gauze, $^{16}O_2$ was pulsed over the catalyst pretreated with $^{18}O_2$ in the same manner as in the case of N_2O decomposition. $^{16}O^{18}O$ and $^{18}O_2$ were detected at the reactor outlet as the products of oxygen isotopic exchange. The main product of oxygen isotopic exchange was $^{16}O^{18}O$. Normalized transient responses of $^{16}O_2$ pulsed as well as isotopes formed in the isotopic exchange reaction ($^{16}O^{18}O$ and $^{18}O_2$) are presented in Fig. 8. The order of appearance of these transient responses reflects a subsequent formation of $^{16}O^{18}O$ and $^{18}O_2$. In contrast to the above

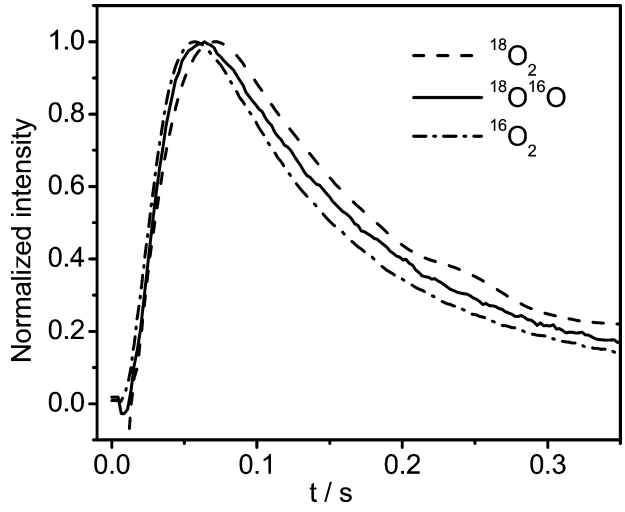

Fig. 8. Normalized transient responses of $^{16}O_2$, $^{18}O^{16}O$, and $^{18}O_2$ when $^{16}O_2$ was pulsed at 973 K over Pt gauze pretreated by $^{18}O_2$.

results on N_2O decomposition over Pt gauze pretreated by $^{18}O_2$ (Fig. 7), the molar fractions of both isotopes increase with an increase in temperature (Fig. 9).

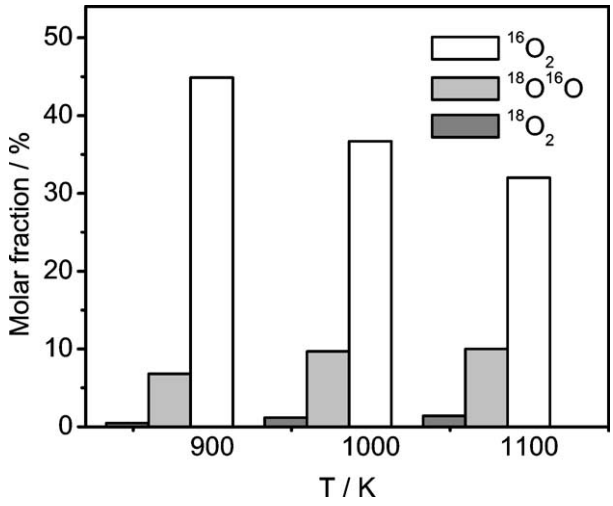

Fig. 9. Molar fractions of $^{16}O_2$, $^{18}O^{16}O$ and $^{18}O_2$ when $^{16}O_2$ was pulsed at different temperatures over Pt gauze pretreated by $^{18}O_2$.

4. Discussion

4.1. Pathways of N_2O decomposition

Discrimination among various kinetic models has revealed that the best description of the experimental data is achieved by model 7, which then confirms on the basis of more information the model proposed by Riekert et al. [6] previously. This model [Eqs. (4)–(7)] suggests the formation of gas-phase oxygen via interaction of N_2O with adsorbed atomic oxygen species [Eq. (5)]. The experiments with isotopically labeled oxygen (see Transient isotopic experiments) reveal the differences in the processes, which lead to redistribution of labeled oxygen in gas-phase when $^{16}O_2$ and $N_2{}^{16}O$ were pulsed over Pt covered with labeled oxygen (^{18}O). To our point of view these results allow an assessment between the various mechanisms suggested in the literature.

For the oxygen isotopic exchange on different Pt catalysts [21,22] various mechanisms have been proposed. For the temperature range from 750 to 800 K and an oxygen pressure of 13 Pa [22], conditions comparable with those in the present study, oxygen isotopic exchange was suggested to proceed via an adsorption/desorption mechanism:

$$^{18}O_2 + 2s \rightleftarrows 2\,{}^{18}O\text{–}s, \tag{9}$$

$$^{18}O\text{–}s + {}^{16}O\text{–}s \rightleftarrows {}^{16}O^{18}O. \tag{10}$$

These equations illustrate formation of O_2 according to the Langmuir–Hinshelwood mechanism for N_2O decomposition [Eq. (3)]. If these reaction pathways would be valid for N_2O decomposition, there ought to be no differences in the order of appearance of oxygen isotopes during N_2O decomposition and oxygen isotopic exchange. However, respective experimental data presented in Figs. 6 and 8 differ significantly. Transient responses of oxygen isotopes ($^{16}O^{18}O$ and $^{16}O_2$) formed during N_2O decomposition over Pt gauze pretreated with $^{18}O_2$ have the same shape and position of maxima (Fig. 6), while transient responses of oxygen isotopes formed during oxygen isotopic exchange are shifted to each other (Fig. 8). Taking into account the reaction pathway for oxygen formation assumed by model 7, the same shape (Fig. 6) of transient responses of isotopically labeled oxygen ($^{16}O^{18}O$ and $^{16}O_2$) can be explained only, when the formation of adsorbed oxygen species from N_2O [Eq. (11)] is fast enough ascertaining no delay in the formation of $^{16}O_2$ [Eq. (12)] as compared to the formation of $^{18}O^{16}O$ from adsorbed ^{18}O–s species [Eq. (13)], which are already present on the surface before N_2O pulsing:

$$N_2{}^{16}O + s \rightarrow N_2 + {}^{16}O\text{–}s, \tag{11}$$

$$N_2{}^{16}O + {}^{16}O\text{–}s \rightarrow N_2 + {}^{16}O_2 + s, \tag{12}$$

$$N_2{}^{16}O + {}^{18}O\text{–}s \rightarrow N_2 + {}^{16}O^{18}O + s. \tag{13}$$

With an increase in temperature the amount of ^{16}O–s formed via interaction of N_2O with Pt atoms [Eq. (11)] increases. A further reaction of these species with N_2O results in an increase in the molar fraction of gas-phase $^{16}O_2$ (Fig. 7). The absence of a respective increase of the molar fraction of $^{16}O^{18}O$ due to the process described by Eq. (13) is surprising because the amount of ^{18}O–s stored on the surface after pretreatment is high enough according to the amount of ^{18}O-containing products formed in the oxygen isotopic exchange reaction. This difference, however, can be explained assuming that not all oxygen species formed by $^{18}O_2$ pretreatment are able to react with N_2O. It is also very important to note that in comparison to the above oxygen pulse experiments, no measurable amount of $^{18}O_2$ was observed on pulsing N_2O over Pt gauze, which had been pretreated by $^{18}O_2$. This observation indicates that recombination of two surface oxygen atoms is not relevant under our conditions. Otherwise there would be no differences in the formation of $^{18}O_2$ on pulsing $^{16}O_2$ or $N_2{}^{16}O$ over the gauze, which had been pretreated by $^{18}O_2$.

The experimentally observed inhibition of N_2O decomposition by gas-phase molecular oxygen (Fig. 2) is also considered in the selected model 7, which predicts an inhibiting effect of oxygen on N_2O decomposition due to competition between gas-phase N_2O and O_2 for the same adsorption sites [Eqs. (4) and (6), respectively]. Such an inhibiting effect of oxygen on the decomposition of nitrous oxide has been previously found for different Pt-containing materials such as wires [7,9,10], foils [5], and sponges [11] under steady-state conditions. However, under transient conditions of the present study, the decrease in N_2O conversion in the presence of gas-phase oxygen is lower as compared to the previous studies, where at least a twofold decrease in the rate of N_2O decomposition was observed at 1273 K when oxygen was added to an N_2O-containing mixture in the proportion 1:1 [7]. This difference can be explained by the fact that under transient conditions in vacuum only a part of the active sites is involved in the reaction due to the small amount of molecules pulsed. In our study this amount was approximately 3×10^{14} molecules per pulse. Under such conditions,

at which the number of molecules pulsed is lower than the number of active sites ($\sim 2 \times 10^{15}$ Pt atoms) the inhibiting effect of gas-phase oxygen should be lower than at ambient pressure.

4.2. Activation energies of the N_2O decomposition pathways

The activation energies for N_2O decomposition over reduced Pt sites [Eq. (9)] as well as for interaction of N_2O with adsorbed oxygen atoms [Eq. (10)] were found to be 81 and 173 kJ mol^{-1}, respectively (Table 2). Apparent activation energies for N_2O decomposition reported in literature for Pt wires [4,9,10] are in the range from 136 to 151 kJ mol^{-1}. However, a direct comparison is not possible because the literature values were calculated assuming a rate-limiting reaction step (recombination of two adsorbed oxygen species formed from N_2O). For this assumption the observed activation energies are a result of the "averaged" contribution of various elementary reaction steps.

For comparison of activation energies of oxygen interaction with Pt gauze derived in this study, literature data, which were obtained under similar experimental conditions, are taken into consideration. Since no high coverage by adsorbed oxygen species exists under transient conditions due to the small amounts of molecules pulsed the choice of literature data was limited to investigations, which deal with coadsorbed molecular and atomic oxygen species at low total coverage. In the present study a higher barrier of 21 kJ mol^{-1} for O_2 adsorption was obtained than the value of 7.4 kJ mol^{-1} reported in [25]. The difference is probably due to the fact that in the latter study the molecular oxygen was adsorbed on a clean Pt (111) surface. However, the respective activation energy may also depend on the degree of coverage by adsorbed oxygen species.

Gland et al. [23] have reported that on a clean Pt (111) surface the activation energy for O_2 desorption was 37 kJ mol^{-1}, while in the presence of an O (2×2) layer the value decreased to 16 kJ mol^{-1}. The activation energy derived from fitting of transient responses in the present study is 10 kJ mol^{-1}. This value is lower than the above values. For dissociation of adsorbed molecular oxygen, the activation energy was reported to be 29 kJ mol^{-1} [24]. This value is very close to the activation energy of 31 kJ mol^{-1}, found for the step O_2–s + s $\xrightarrow{k_5}$ 2O–s in this study. Thus, the activation energies for N_2O decomposition and oxygen interaction with Pt gauze obtained in this study are in relatively good agreement with literature data.

5. Conclusions

A mechanistic scheme and kinetic parameters of the catalytic decomposition of N_2O over knitted Pt gauze under transient conditions were derived on the basis of experiments with isotopic labeled molecules and results of simultaneous fitting of the transient responses of N_2O, N_2, and O_2 to different kinetic models and discrimination among them. The best description of experimental data was achieved assuming the formation of gas-phase molecular oxygen mainly due to interaction of adsorbed oxygen species with gas-phase N_2O. Adsorbed oxygen species are formed via interaction of gas-phase N_2O with Pt metallic sites as well as by dissociative oxygen adsorption via a molecular precursor. The rate of recombination of two adsorbed oxygen atoms was assumed to be slow under the transient conditions. The inhibiting effect of gas-phase molecular oxygen on N_2O decomposition, observed in the present study, was explained in the frame of the evaluated mechanistic scheme by competition between gas-phase N_2O and O_2 for the same active sites.

Acknowledgments

V. Kondratenko thanks ACA (Institute for Applied Chemistry Berlin–Adlershof) for a fellowship during her PhD work. Financial support by Deutsche Forschungsgemeinschaft within the frame of the priority program "Bridging the gap between real and ideal systems in heterogeneous catalysis" SPP 1091 has also been greatly appreciated. Assistance of Fonds der Chemische Industrie is also recognized.

References

[1] M.A. Wojtowicz, J.R. Pels, J.A. Moulijn, Fuel Process. Technol. 34 (1993) 1.
[2] W.C. Trogler, J. Chem. Educ. 72 (1995) 973.
[3] F. Kapteijn, J. Rodriguez-Mirasol, J.A. Moulijn, Appl. Catal. B 9 (1996) 25.
[4] C.N. Hinshelwood, C.R. Prichard, J. Chem. Soc. 127 (1925) 327.
[5] L. Riekert, M. Staib, Z. Electrochem. 66 (1962) 735.
[6] L. Riekert, M. Staib, Ben. Bunsen-Ges. Phys. Chem. 67 (1963) 976.
[7] L. Riekert, D. Menzel, M. Staib, Proc. 3rd Intl. Congr. Catal. 1 (1965) 387.
[8] H.-G. Lintz, L. Riekert, Z. Phys. Chem. 42 (1–2) (1964) 87.
[9] C.G. Takoudis, L.D. Schmidt, J. Catal. 80 (1983) 274.
[10] G.A. Papapolymerou, L.D. Schmidt, Langmuir 1 (1985) 488.
[11] E.W.R. Steacie, J.W. McCubbin, J. Chem. Phys. 2 (1934) 585.
[12] J.T. Gleaves, J.R. Ebner, T.C. Kuechler, Catal. Rev.-Sci. Eng. 30 (1988) 49.
[13] J.T. Gleaves, G.S. Yablonsky, P. Phanawadee, Y. Schuurman, Appl. Catal. A 160 (1997) 55.
[14] M. Soick, D. Wolf, M. Baerns, Chem. Eng. Sci. 55 (2000) 2875.
[15] E.V. Kondratenko, O.V. Buyevskaya, M. Baerns, J. Mol. Catal. A 158 (2000) 199.
[16] C.G. Takoudis, L.D. Schmidt, J. Catal. 84 (1983) 235.
[17] S. Tanaka, K. Yuzaki, S. Ito, H. Uetzuka, S. Kameoka, K. Kunimori, Catal. Today 63 (2000) 413.
[18] Y. Ohno, I. Kobal, H. Horino, I. Rzeznicka, T. Matsushima, Appl. Surf. Sci. 169–170 (2001) 273.
[19] N.R. Avery, Surf. Sci. 131 (1983) 501.
[20] E.W.R. Steacie, J.W. McCubbin, Can. J. Res. B 14 (1936) 84.
[21] Y.L. Sandler, D.B. Durigon, J. Phys. Chem. 1968 (1968) 1051.
[22] V.I. Sobolev, V.A. Sobyanin, A.V. Pashis, A.V. Kalinkin, G.I. Panov, Surf. Sci. 173 (1986) 498.
[23] J.L. Gland, B.A. Sexton, G.B. Fischer, Surf. Sci. 95 (1980) 587.
[24] J.L. Gland, Surf. Sci. 93 (1980) 487.
[25] A.-P. Egl, F. Eisert, A. Rosen, Surf. Sci. 382 (1997) 57.